SAND2014-4915C

Characterizing Populations, Predicting Presence & Examining Mechanical Response Using 3D Reconstructions of Porosity in Laser Welds

Exceptional service in the national interest

Sandia National Laboratories

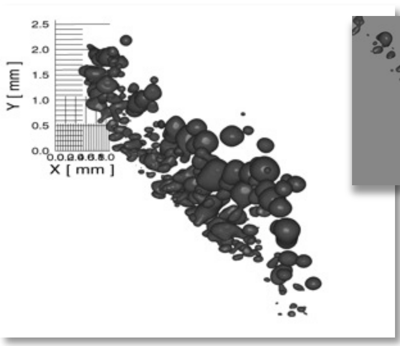

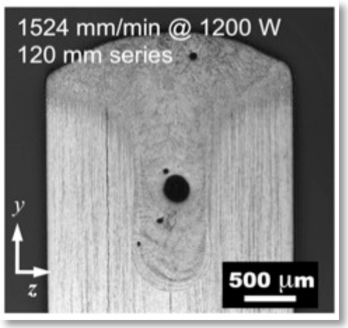

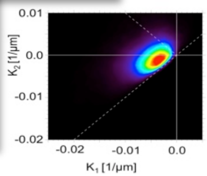

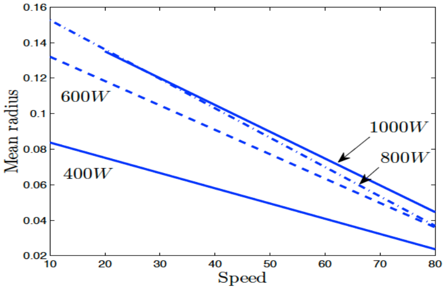

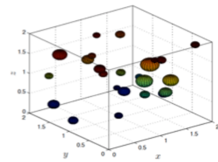

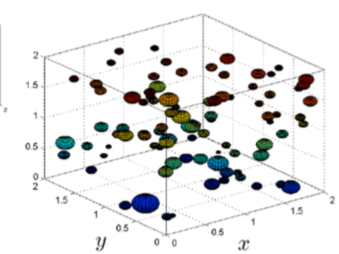

J. Madison[1], C.C. Battaile[1], J. Rodelas[1], J. Foulk[2], T. Payton[3], L.K. Aagesen[4], V.W.L. Chan[4], K. Thornton[4], M. Grigoriu[4]

[1] Sandia National Laboratories – NM
[2] Sandia National Laboratories – CA
[3] NM Institute of Technology
[4] University of Michigan
[5] Cornell University

The 2nd International Conference on 3DMS 3D Materials Science 2014

U.S. DEPARTMENT OF ENERGY

NNSA National Nuclear Security Administration

Sandia National Laboratories is a multi-program laboratory managed and operated by Sandia Corporation, a wholly owned subsidiary of Lockheed Martin Corporation, for the U.S. Department of Energy's National Nuclear Security Administration under contract DE-AC04-94AL85000.
SAND No. 2014-XXXX.

Acknowledgements

- Sandia National Laboratories, Albuquerque, NM
  - Danny O. MacCallum, Org. 1831 – Multiscale Metallurgical S&T
  - Joseph A. Romero, Org. 1522 – Experimental NDE & Model Validation
  - Burke L. Kernen, Org. 1522 – Experimental NDE & Model Validation
  - Ciji Nelson, Org. 1522 – Experimental NDE & Model Validation
  - Alice Kilgo, Org. 1822 – Materials Characterization
  - James Foulk, III, Org. 8256 – Mechanics of Materials
  - Helena Jin, Org. 1814 – Computational Materials
- Naval Research Laboratory
  - Dave Rowenhorst, Multifunctional Materials Division
- Northwestern University
  - Voorhees Group – Materials Science & Engineering
- Sandia National Laboratories, Early Career LDRD Award

Laboratory Directed Research & Development

Outline

Sandia National Laboratories

- Background
  - SNL Interest in Welds & Joinings
  - Laser Welding – Process & Challenges
- Characterization Results
  - μ−Computed Tomography
  - Porosity Trends & Distributions
  - Interfacial Measures (ISD, IND)
  - Pore Interspacing
- Predictive Probabilistic Model
- Modeling Mechanical Response
- Summary

SNL Interest in Welds & Joinings

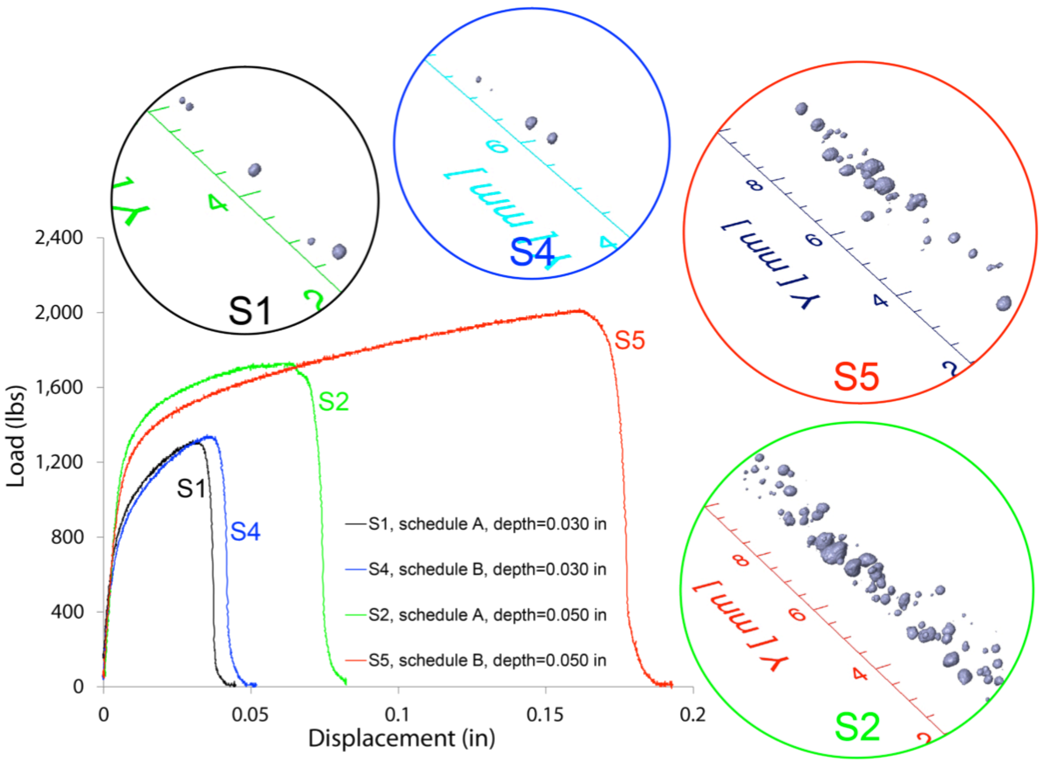

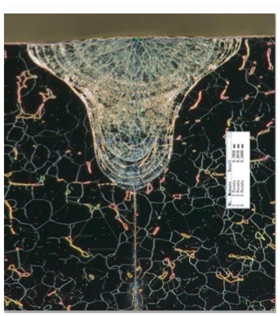

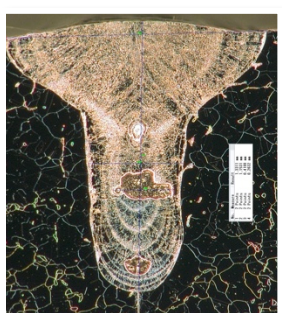

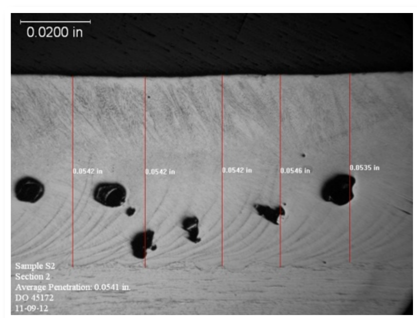

- M. Cieslak, A. Ritter, *"Precipitate Formation in Austenitic Stainless Steel Welds,"* **Scripta Met**., Vol. 19, Issue 2, (1985) pp. 165-168
- J. Jellison, M. Cieslak, *Laser Materials Processing at Sandia National Laboratories,* presented at Applications of Lasers and Electro-Optics, Orlando FL, October 1994
- G. Knorovsky, M. Kanouff, P. Fuerschbach, D. Noble, P. Schunk, D. MacCallum, F. Hooper, *Calculated Versus Experimental Heat Inputs in Laser Spot Welding,* presented at The American Welding Society, Chicago IL, April 2000
- C. Robino, A. Hall, J. Brooks, T. Headley, R. Roach, **SAND2002-4014** : Solidification Diagnostics for Joining and Microstructural Simulations, January 2003
- V. Semak, G. Knorovsky, D. MacCallum, R. Roach, *"Effect of Surface Tension on Melt Pool Dynamics During Laser Pulse Interaction,"* **J. Phys. D: Appl. Phys.** Vol. 39, (2006) pp. 590-595
- *Boyce, Reu & Robino, "The Constitutive Behavior of Laser Welds in 304L Stainless Steel Determined by Digital Image Correlation,"* ***Met Trans A,*** *Vol. 37A (2006) pp. 2481-2492*
- J. Norris, M. Perricone, R. Roach, K. Faraone & C. Ellison, **SAND2007-1051** : Evaluation of Weld Porosity in Laser Beam Seam Welds: Optimizing Continuous Wave and Square Wave Modulated Processes, February 2007
- J. Madison, L.K. Aagesen, *"Quantitative Characterization of Porosity in Laser Welds of Stainless Steel,"* **Scripta Mat.**, Vol. 67, Issue 9, (2012) pp. 783-786.
- J. Madison, L.K. Aagesen, C. Battaile, J. Rodelas, T. Payton, *"Coupling 3D Quantitative Interrogation of Weld Microstructure with 3D Models of Mechanical Response,"* **Metall. Microstr. Anal.**, Vol. 2, Issue 6, (2013) 359-363.

Laser Welding

C	Cr	Cu	Mn	Mo	Ni	N	P	S	Si	Fe
0.03	18.09	0.2	1.73	0.16	8.57	0.06	0.024	0.001	0.36	bal.

304L Stainless Steel (wt%)

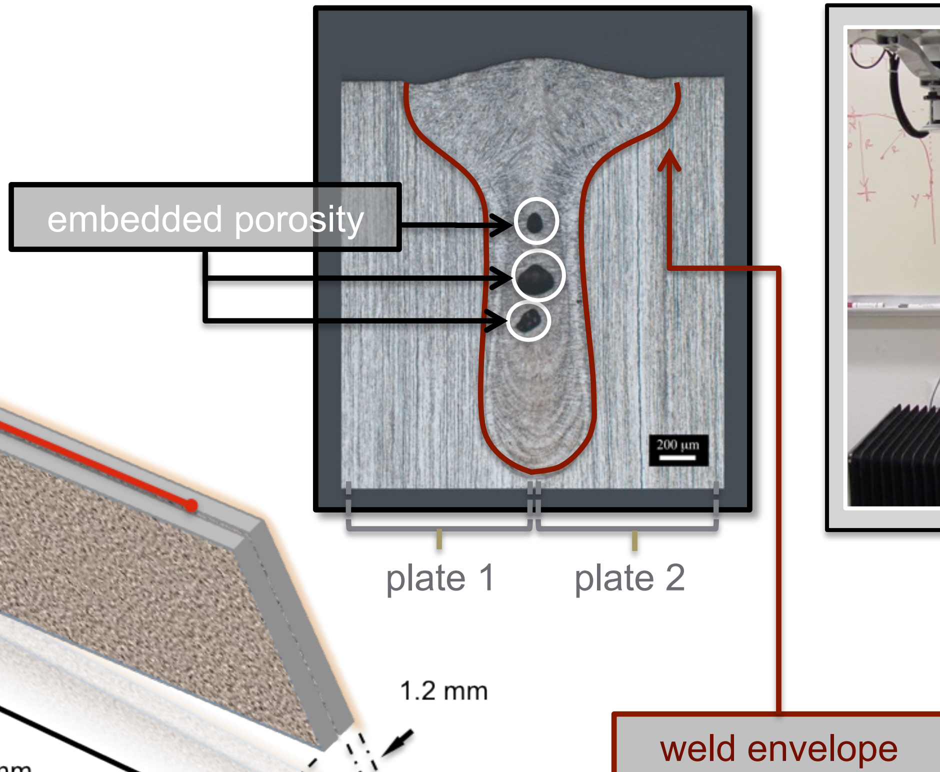

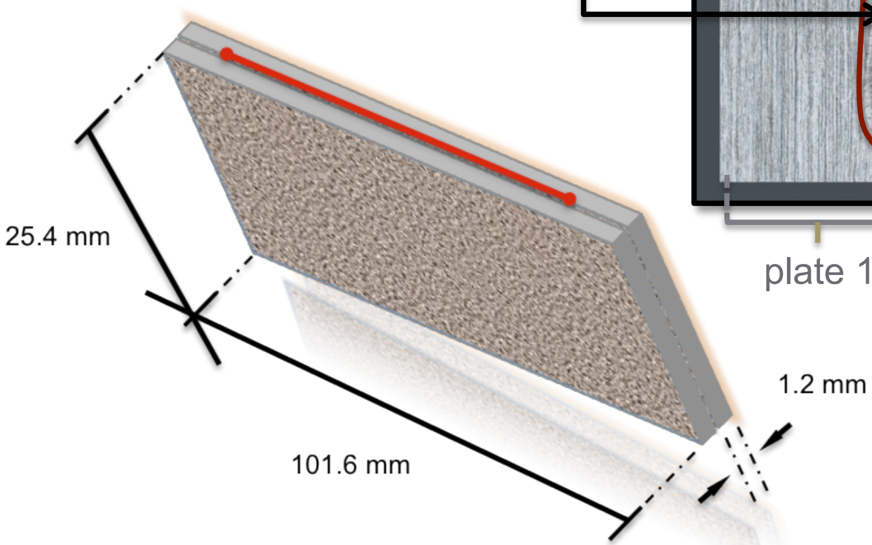

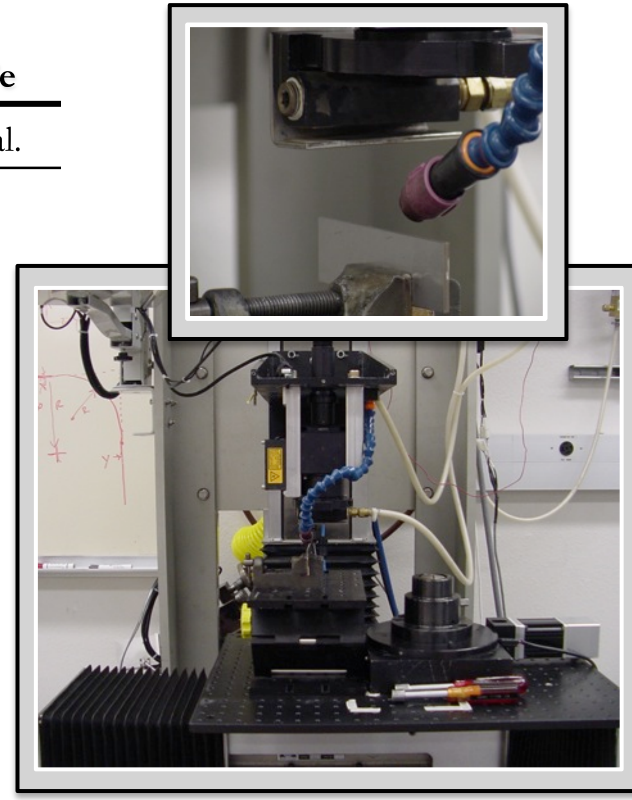

ROFIN SINAR Nd:YAG
- 3-axis stage
- Constant speed
- Ar shielding gas
- CW or PW

μ-Computed Tomography

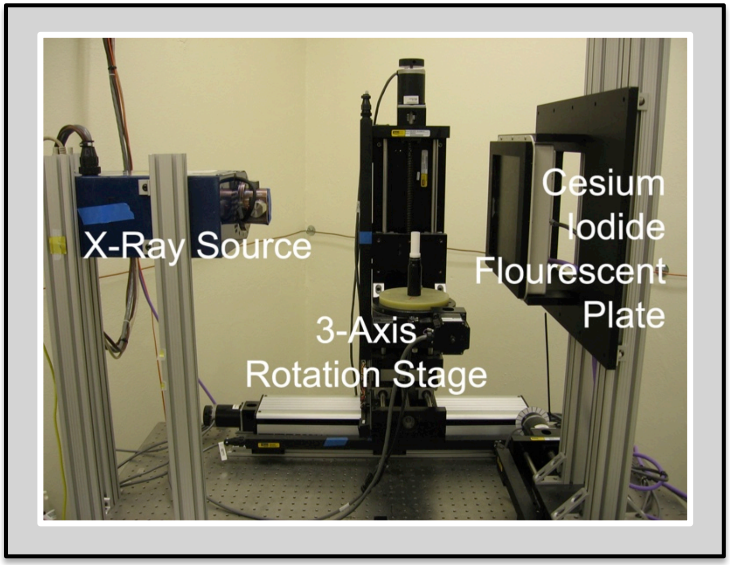

Kevex PSX 10-65W X-ray Tube
Varian 2520 Detector

North Star Imaging, Inc. X50 XViewCT Cabinet System
YXLON Demountable Microfocus Tube

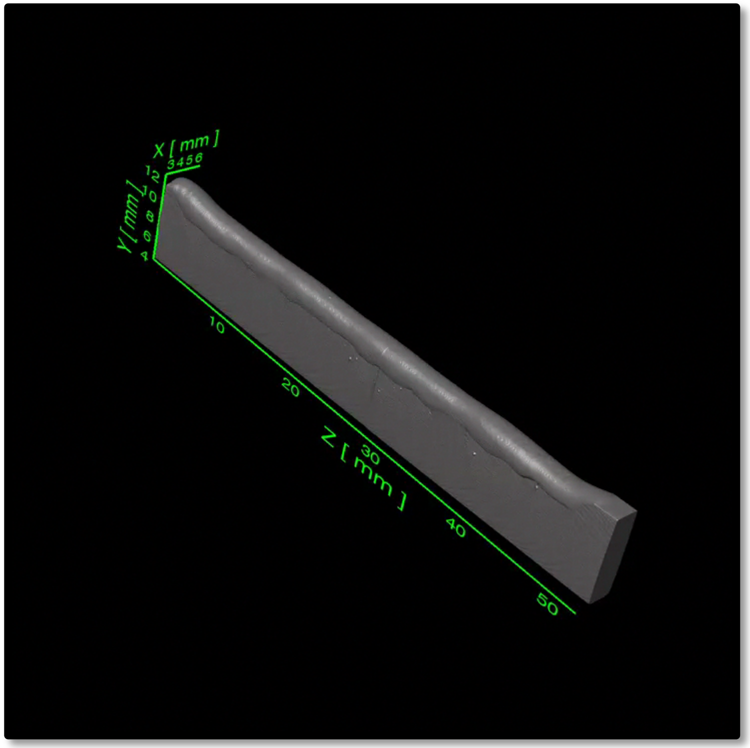

- At SNL we have multiple micro-computed tomography options for experimental chacterization and non-destructive evaluation
- Options present an ability to accommodate various sample sizes and meet various resolution constraints
- 6 powers (200 – 1200 W)
- 5 speeds (200 – 2000 mm x min^{-1})
- 2 focal lenses (80 mm | 120 mm)

Porosity Trends

80 mm lens

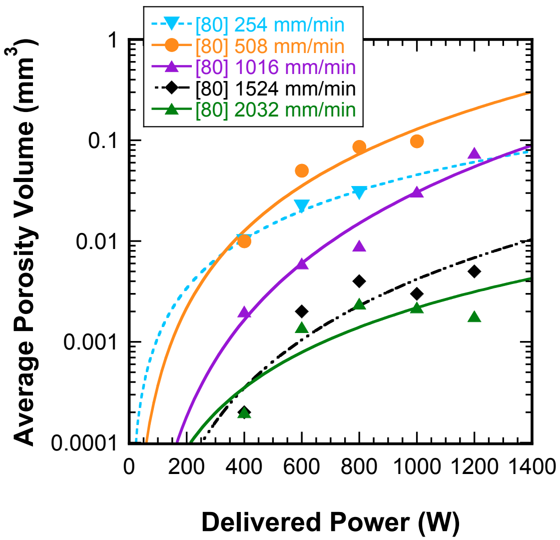

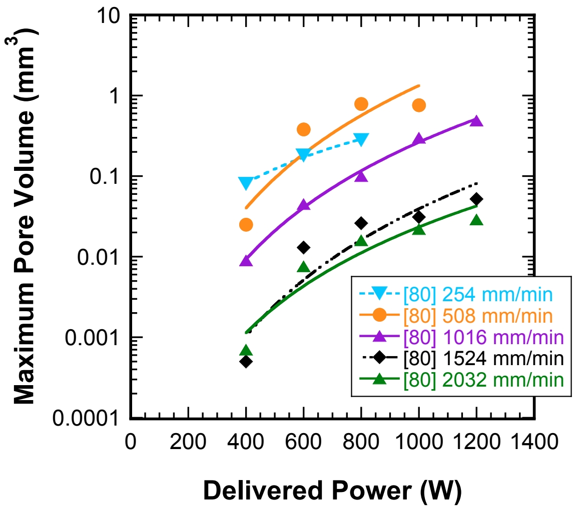

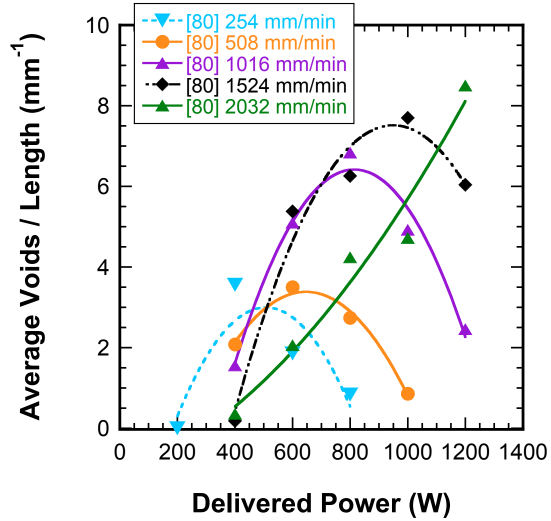

120 mm lens

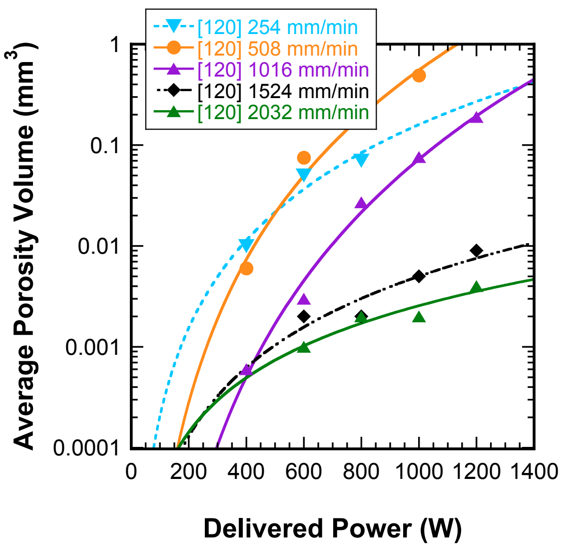

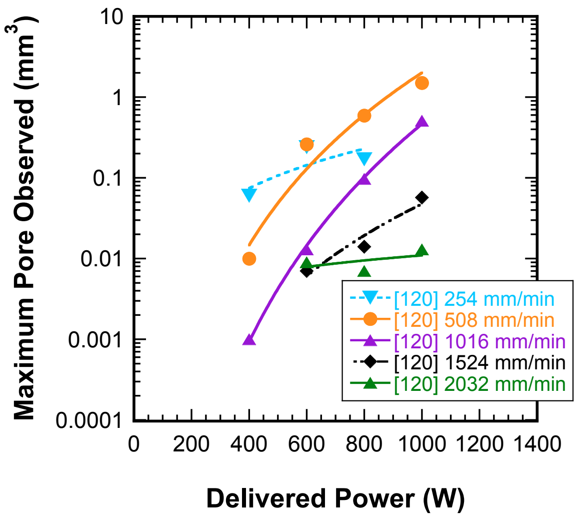

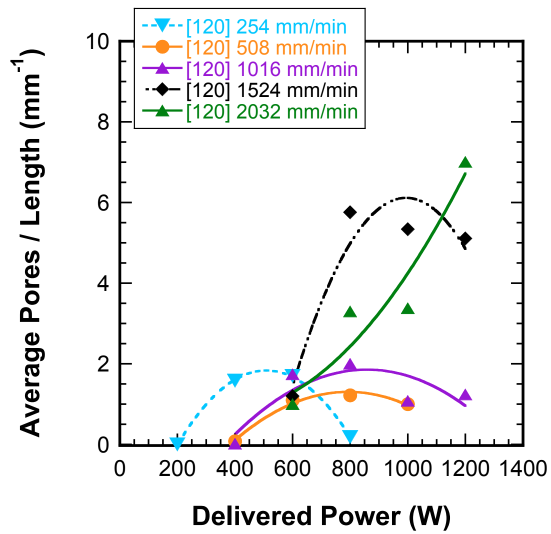

Porosity At First Glance

1016 mm/min

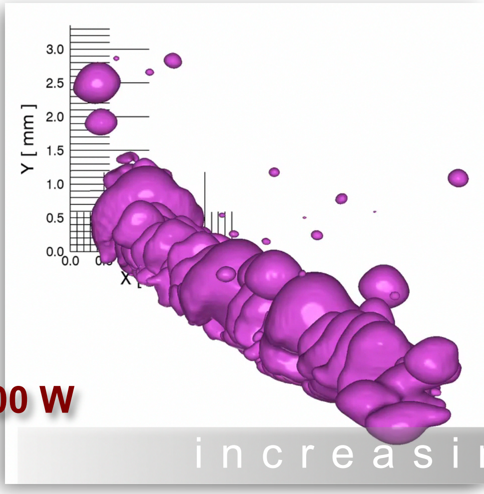

1524 mm/min

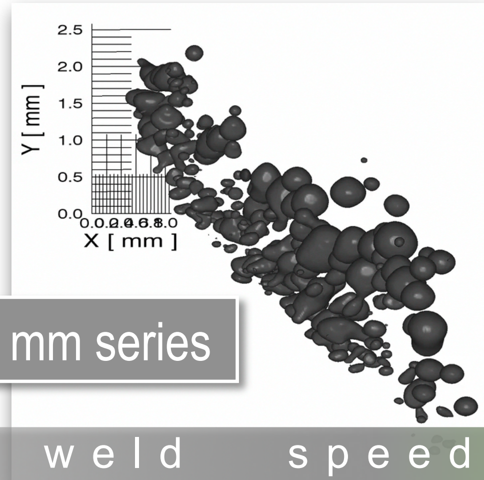

2032 mm/min

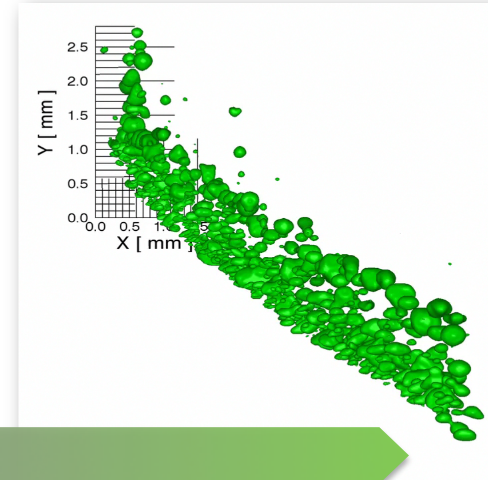

120 mm series

1200 W

increasing weld speed

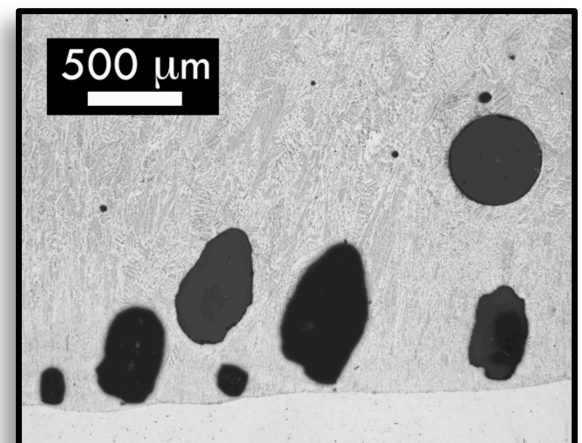

1016 mm/min

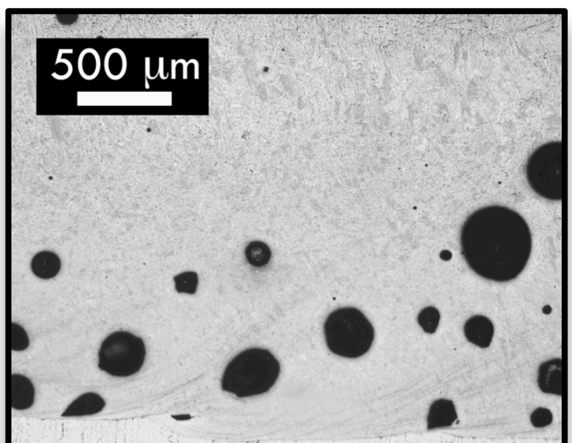

1524 mm/min

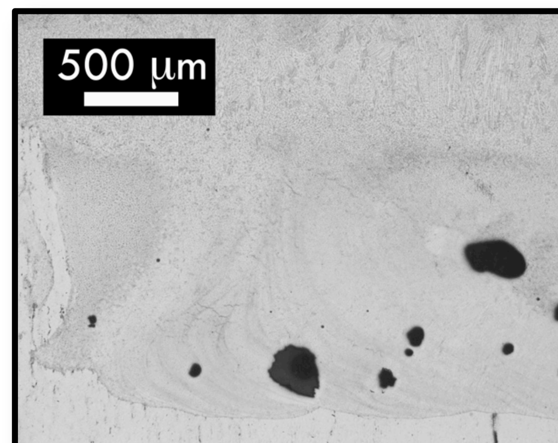

2032 mm/min

*Madison & Aagesen, **Scripta Mat.,** Vol. 67 (2012) pp. 783-786*

Porosity Distributions

1016 mm/min **1524 mm/min** **2032 mm/min**

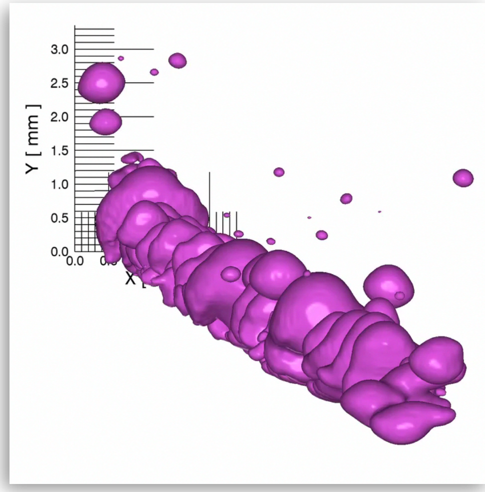

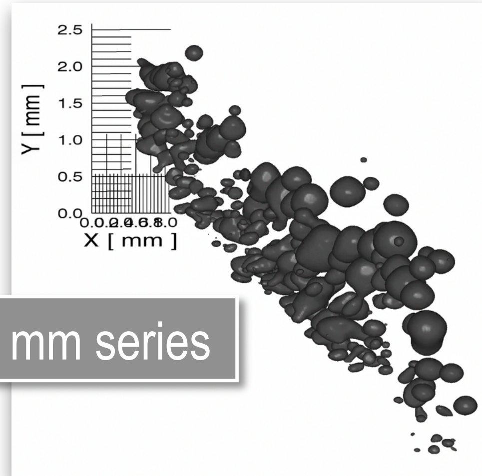

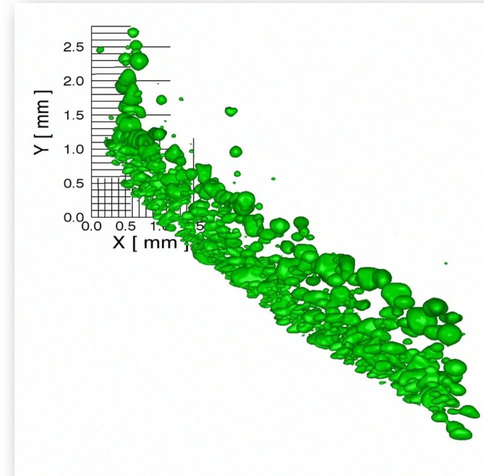

120 mm series

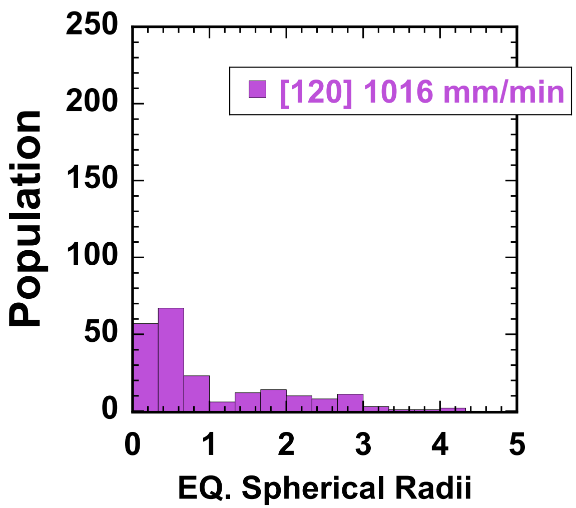

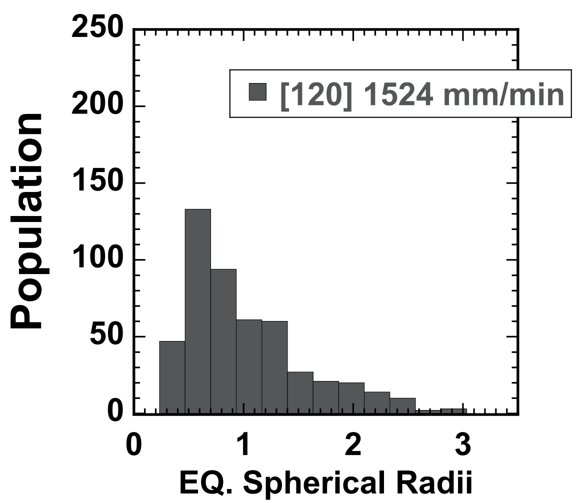

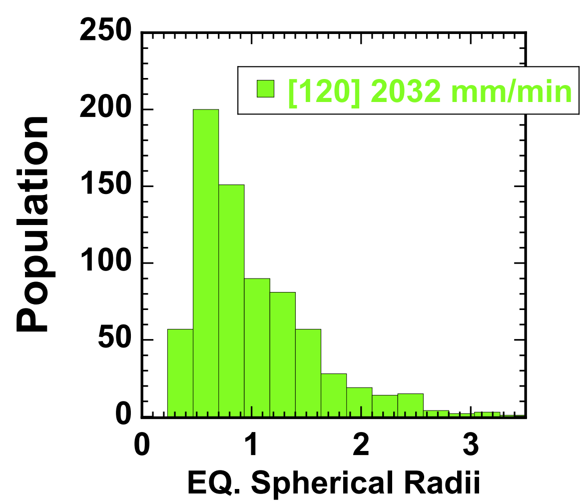

*Madison & Aagesen, **Scripta Mat.,** Vol. 67 (2012) pp. 783-786*

Interfacial Measures

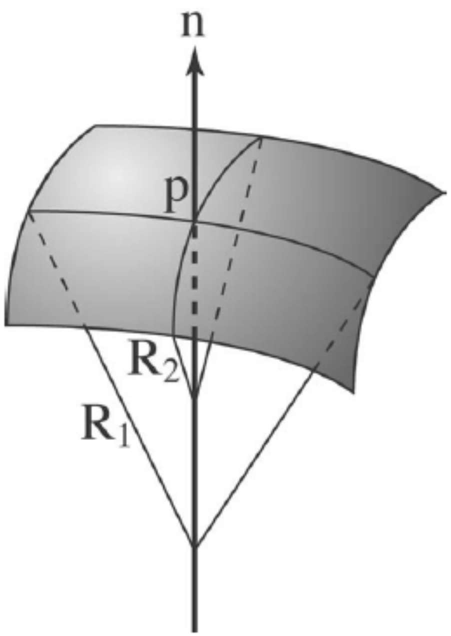

$$H = \frac{1}{2}\left(\frac{1}{R_1} + \frac{1}{R_2}\right)$$

Mean Curvature

$$K = \left(\frac{1}{R_1 R_2}\right)$$

Gaussian Curvature

$$\kappa_1 = H - \sqrt{H^2 - K}$$

$$\kappa_2 = H + \sqrt{H^2 - K}$$

Minimum & Maximum Principle Curvatures

*Alkemper, Voorhees,, **Acta Mater.**, vol. 49 (2001) pp. 897-902.*
R. Mendoza*, et al.*, ***Metall. Mater. Trans. A*,** vol. 34A (2003) pp. 481-489.
*Mendoza, Alkemper & Voorhees, **Met Trans. A,** Vol. 34A (2003) pp. 481-489*
R. Mendoza, *et al*., ***Nat. Mater.*,** vol. 3 (2004) pp. 385-388.
D. Kammer*, et al.*, ***Scripta. Mater.*,** vol. 55 (1) **(**2006),, pp. 17-22.
*Kammer & Voorhees, **Acta Mater.,** vol. 54, (2006) pp. 1549-1558*
*Kammer & Voorhees, **MRS Bull.,** vol. 33, (2008) pp. 603-610*
Fife & Voorhees, ***Acta Mater.***, vol. 57, (2009) pp. 2418-2428

Interfacial Measures

ISD

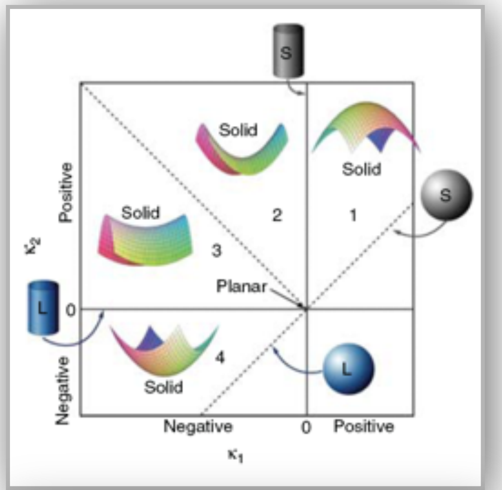

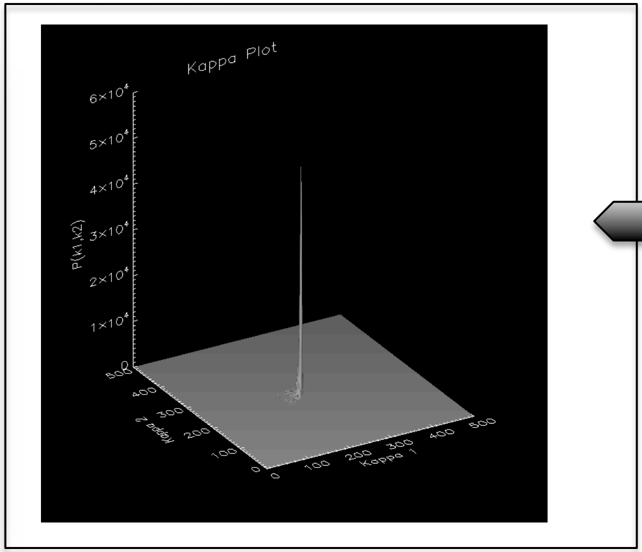

$P(\kappa_1, \kappa_2)$

$P(n)$

IND

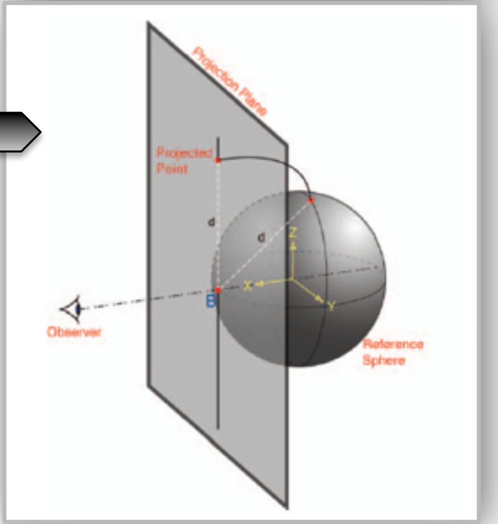

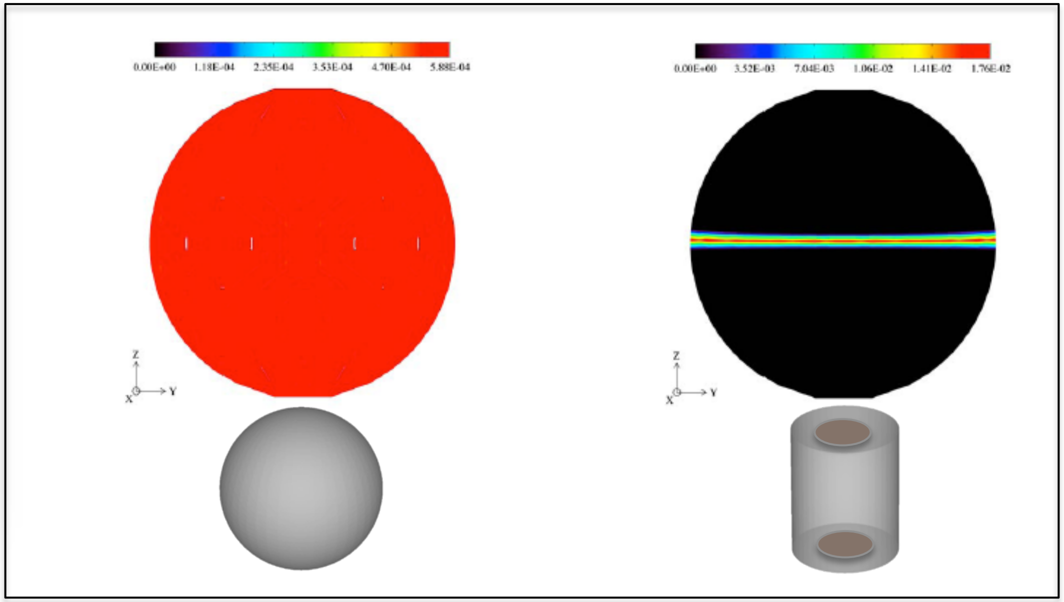

Kammer & Voorhees, ***Acta Mater.***, *vol. 54, (2006) pp. 1549-1558*


1200 W
1000 W
800 W
600 W
400 W
INCREASING POWER DELIVERED
120-1200-40
120-1200-60
120-1200-80
120-1000-20
120-1000-40
120-1000-60
120-1000-80
120-800-10
120-800-20
120-800-40
120-800-60
120-800-80
120-600-10
120-600-20
120-600-40
120-600-60
120-600-80
120-400-10
INCREASING WELD SPEED
120 mm series
3D Reconstructions
254 mm/min
508 mm/min
1016 mm/min
1524 mm/min
2032 mm/min

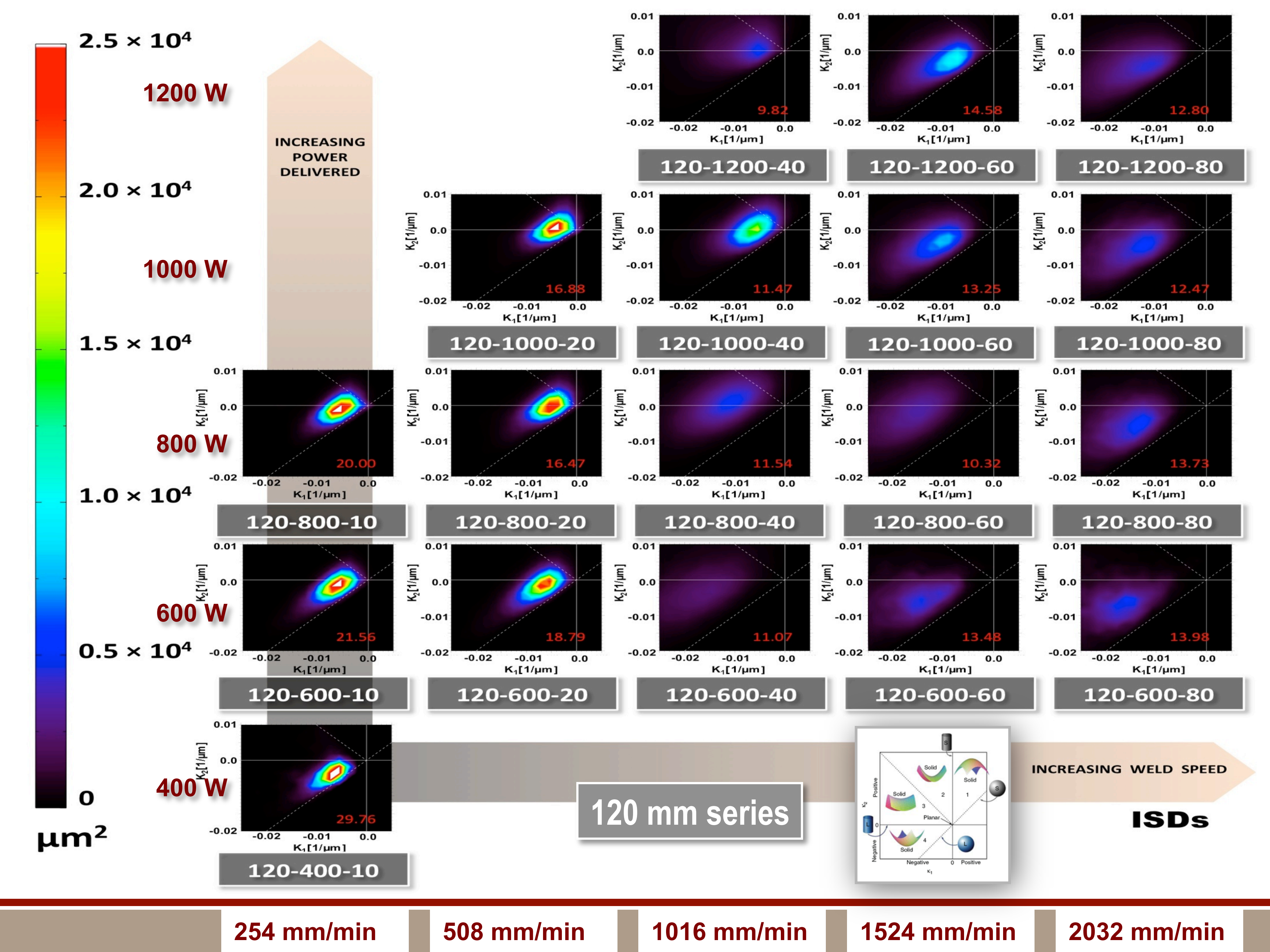
2.5 × 10⁴
2.0 × 10⁴
1.5 × 10⁴
1.0 × 10⁴
0.5 × 10⁴
0
μm²
1200 W
1000 W
800 W
600 W
400 W
INCREASING POWER DELIVERED
K₂[1/μm]
K₁[1/μm]
9.82
120-1200-40
14.58
120-1200-60
12.80
120-1200-80
16.88
120-1000-20
11.47
120-1000-40
13.25
120-1000-60
12.47
120-1000-80
20.00
120-800-10
16.47
120-800-20
11.54
120-800-40
10.32
120-800-60
13.73
120-800-80
21.56
120-600-10
18.79
120-600-20
11.07
120-600-40
13.48
120-600-60
13.98
120-600-80
29.76
120-400-10
120 mm series
INCREASING WELD SPEED
ISDs
254 mm/min
508 mm/min
1016 mm/min
1524 mm/min
2032 mm/min

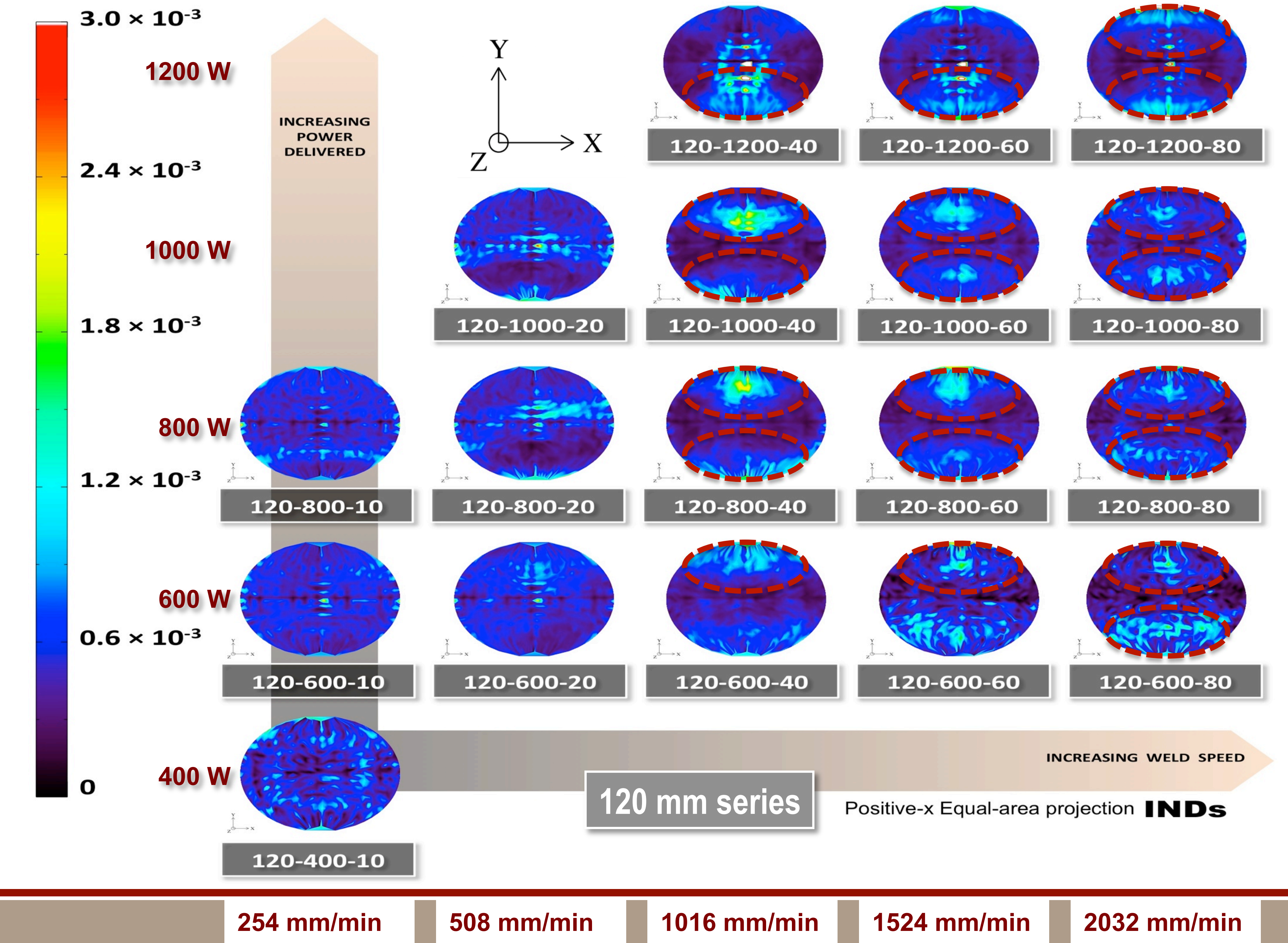
3.0 × 10⁻³
1200 W
2.4 × 10⁻³
1000 W
1.8 × 10⁻³
800 W
1.2 × 10⁻³
600 W
0.6 × 10⁻³
400 W
0
INCREASING POWER DELIVERED
Y
X
Z
120-1200-40
120-1200-60
120-1200-80
120-1000-20
120-1000-40
120-1000-60
120-1000-80
120-800-10
120-800-20
120-800-40
120-800-60
120-800-80
120-600-10
120-600-20
120-600-40
120-600-60
120-600-80
120-400-10
INCREASING WELD SPEED
120 mm series
Positive-x Equal-area projection INDs
254 mm/min
508 mm/min
1016 mm/min
1524 mm/min
2032 mm/min

Pore Interspacing I

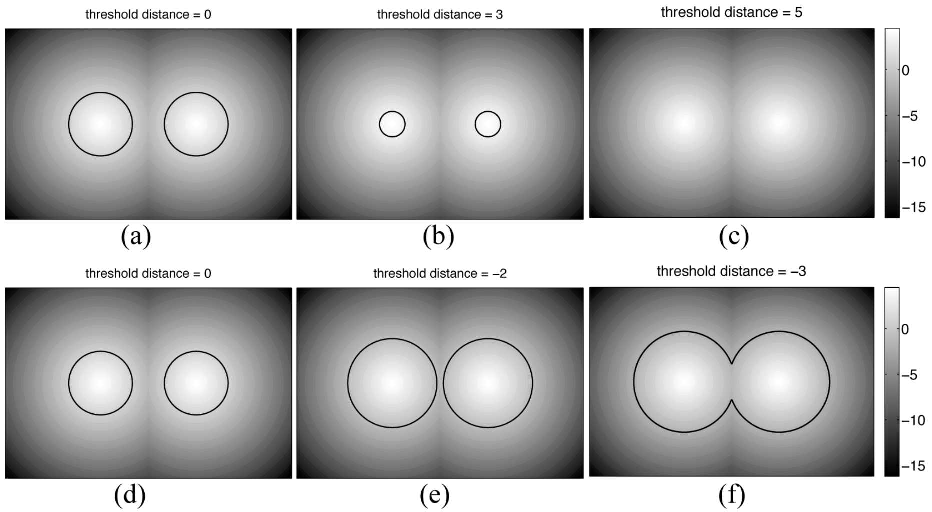

Interfacial Distance Distribution (IDD)

Chan & Thornton, **Acta Mat.**, Vol. 60 (2012) pp. 2509-2517

Pore Interspacing Distribution (PID)

Measures the fraction of pores lying a specific interfacial distance apart by tracking topological changes in 3d under expanding or contracting isosurfaces

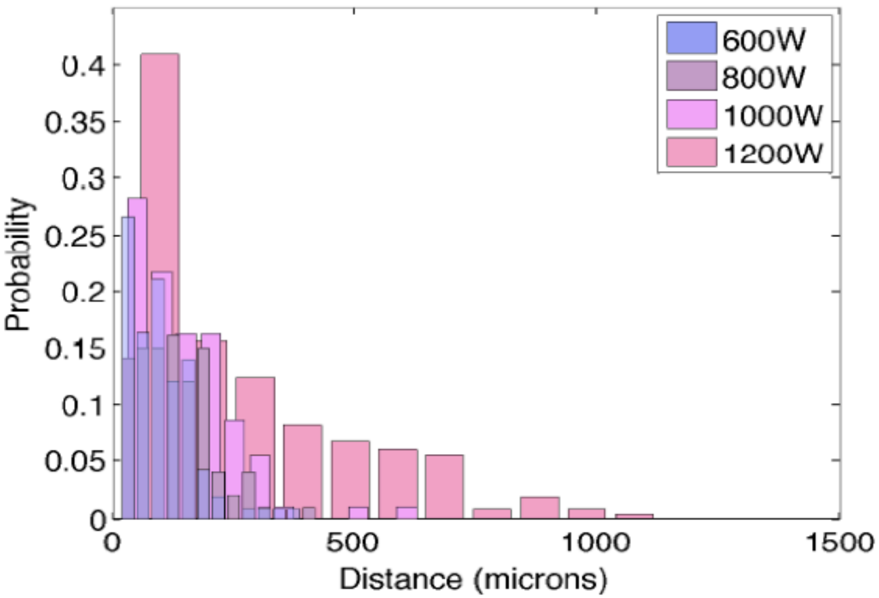

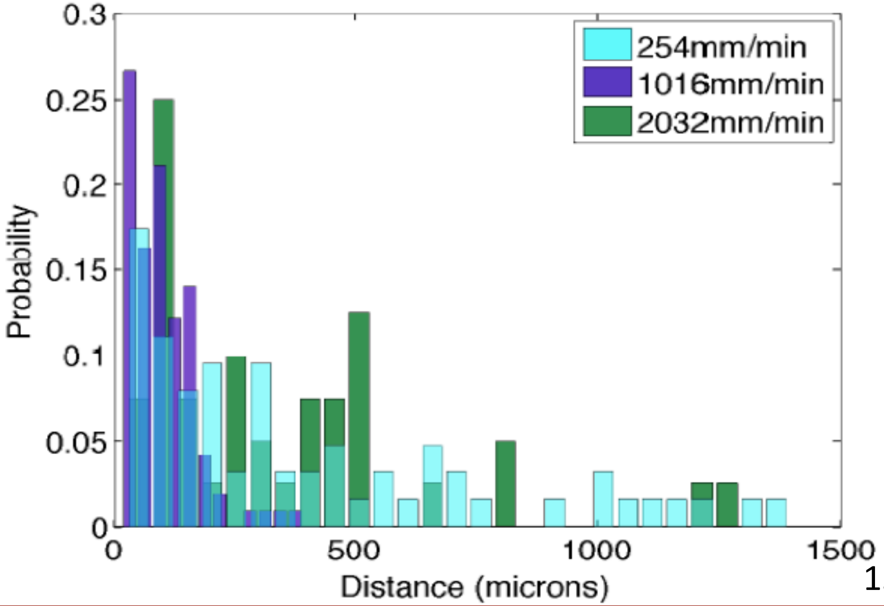

*Madison, Aagesen, Chan, Thornton, **IMMI,** vol. 3 (2014)*

Pore Interspacing II

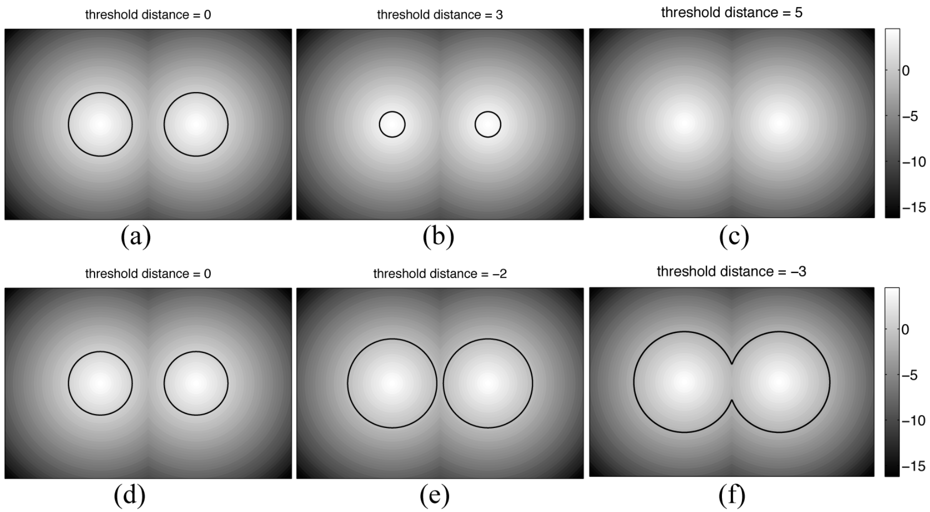

Solid Linear Fraction (SLF)

$$SLF = \frac{R}{r+R} = \frac{\frac{1}{2}(\overline{\mu}_w(PID))}{\mu(r) + \frac{1}{2}(\overline{\mu}_w(PID))}$$

Provides a linear measure of solid fraction between centers of neighboring pores scaled relative to the average pore size

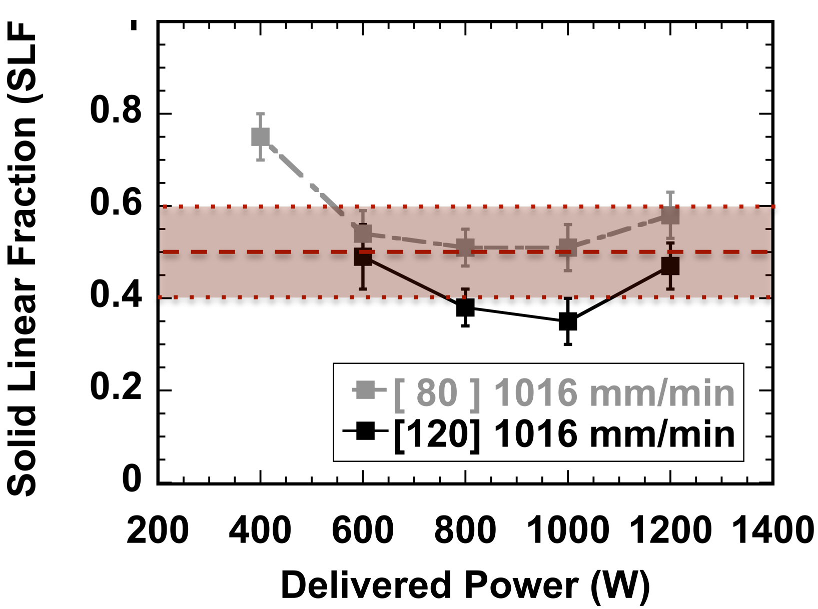

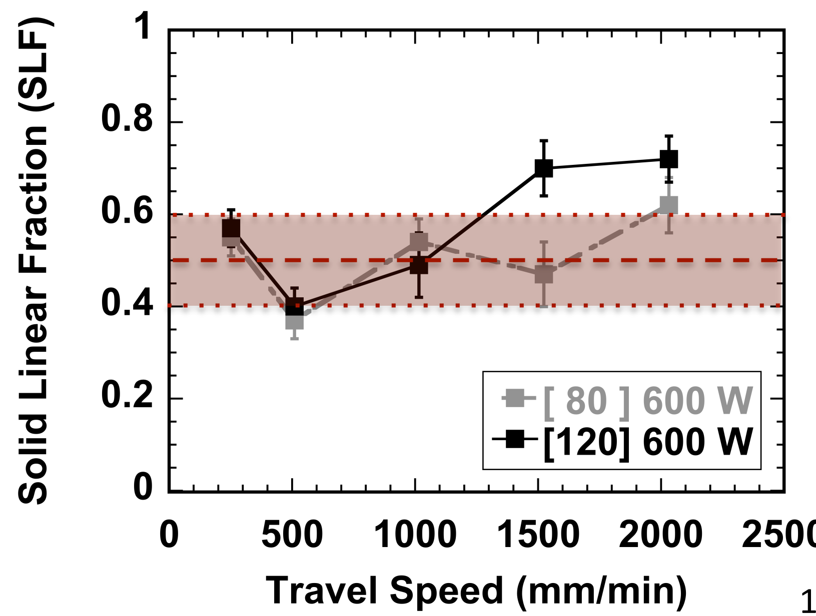

*Madison, Aagesen, Chan, Thornton, **IMMI,** vol. 3 (2014)*

Now what…….

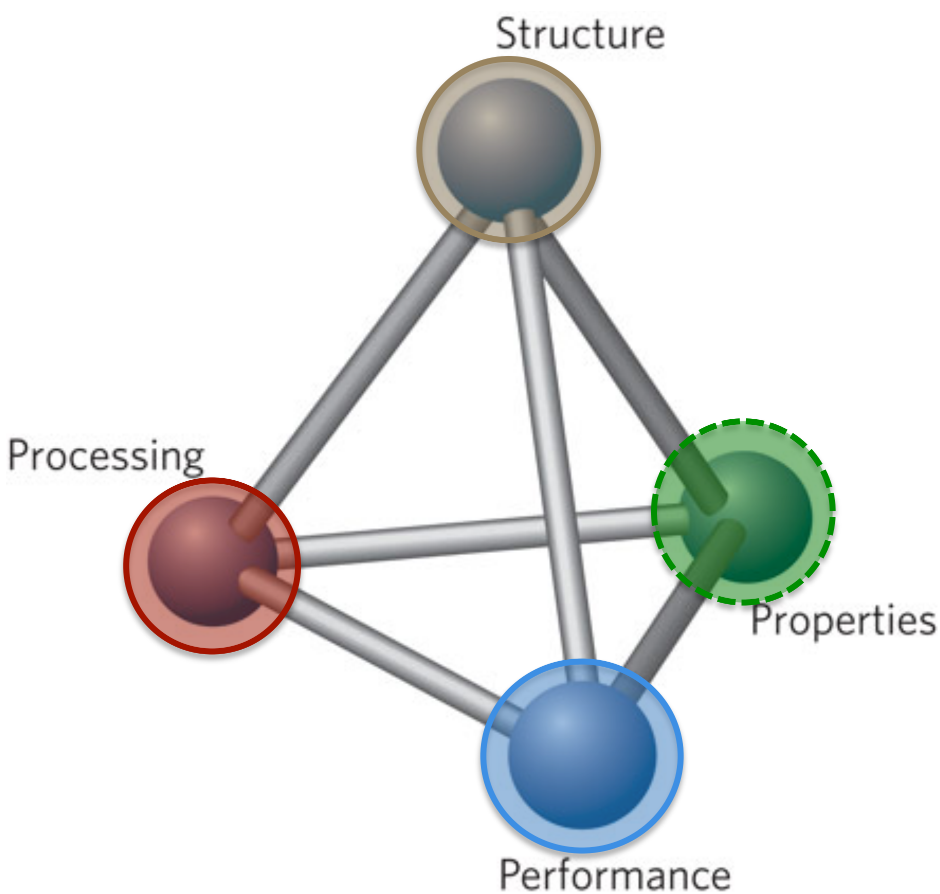

Weld schedule

Average/Max Pore Size
Linear Frequency
Morphology
Directionality
Pore Interspacing
Solid Linear Fraction

Image-based modeling

Tailored finite elements

Synthetic microstructure

Mechanical testing

processing

structure

performance

properties

Pore Prediction

Sandia National Laboratories

Gamma distribution with a shift r_{min} = 0.02mm and
Pore radii = $R = r_{min} + X$ where X is a gamma random variable with shape parameters α, $\beta > 0$ estimated from observation

moment of PDF of X $= E[X^r] = \beta^r \Gamma(\alpha + r) / \Gamma(\alpha) \quad \text{for } r \geq 1$

mean $= \mu_X = \beta\Gamma(\alpha+1)/\Gamma(\alpha) = \alpha\beta$

variance $= \sigma_X^2 = \alpha\beta^2$

coefficient of variation $= \upsilon_X = \sqrt{\sigma_X^2} / \mu_X = \alpha^{-1/2}$

skewness coefficient $= \gamma_{3,X} = \dfrac{E[(X-\mu_X)^3]}{(E[(X-\mu_X)^2])^{3/2}} = 2\alpha^{-1/2}$

$$E[R] = r_{\min} + \mu_X$$
$$\gamma_{3,X} = \gamma_3$$

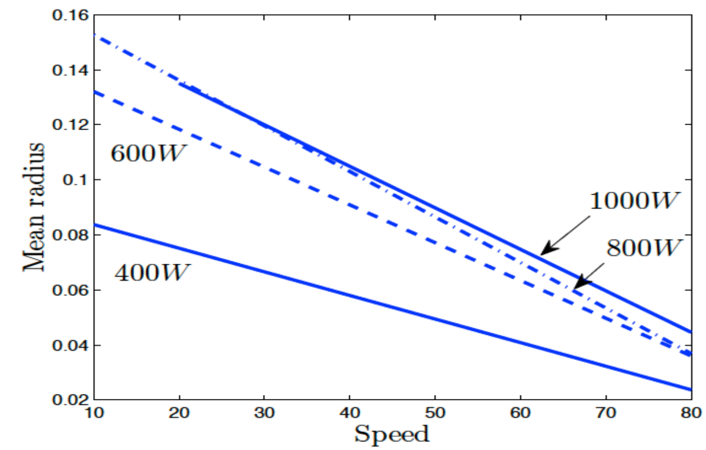

$$r_{mean} = \begin{cases} 0.0923 - 0.0009v \\ 0.1458 - 0.0014v \\ 0.1692 - 0.0017v \\ (0.1652 - 0.0015v)\ (v \geq 20) \end{cases} \qquad \gamma_3 = \begin{cases} 0.6267, & \text{for } 400W \\ 0.8735, & \text{for } 600W \\ 0.9784, & \text{for } 800W \\ 0.9359, & \text{for } 1000W \end{cases}$$

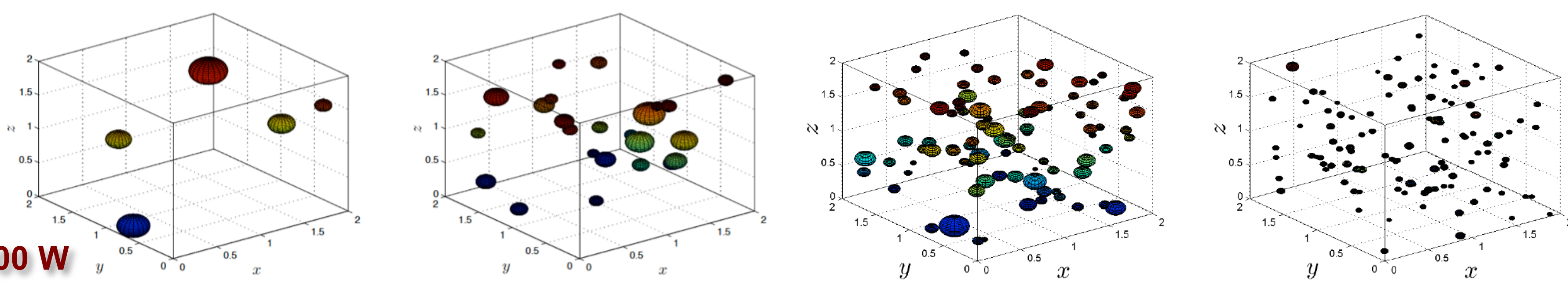

600 W

increasing weld speed

508 mm/min	1016 mm/min	1524 mm/min	2032 mm/min

Mechanical Response I

Explicit microstructure

Jas3D

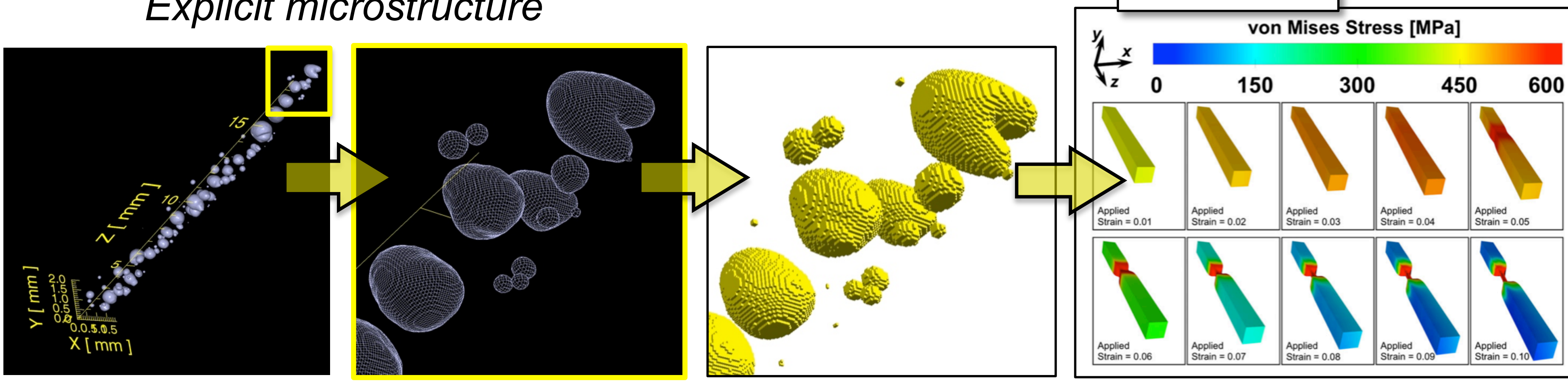

We explicitly embed the 3d microstructure obtained via μCT into a F.E.A. environment to examine local and global strain behavior and compare this to tensile tests of the actual microstructures

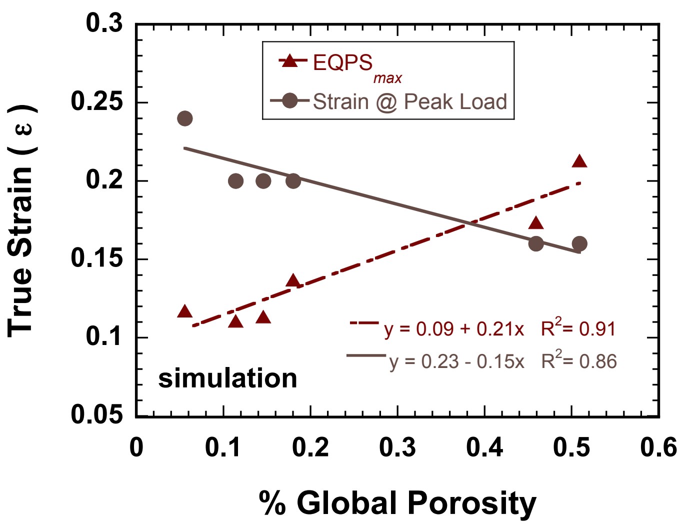

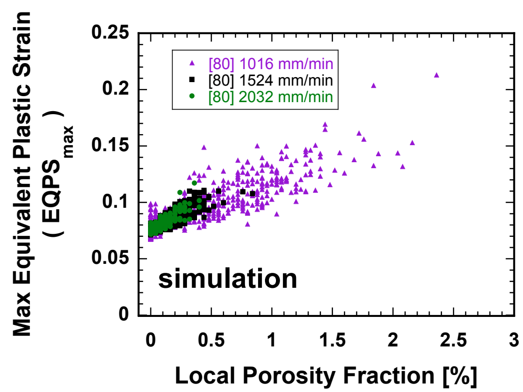

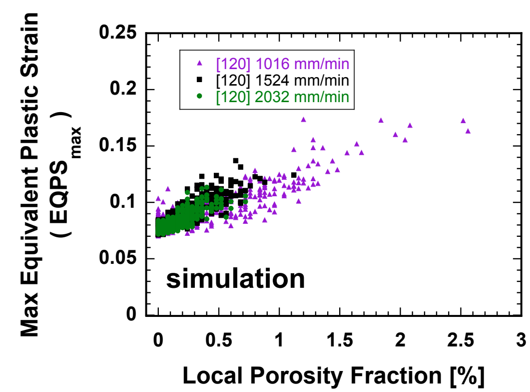

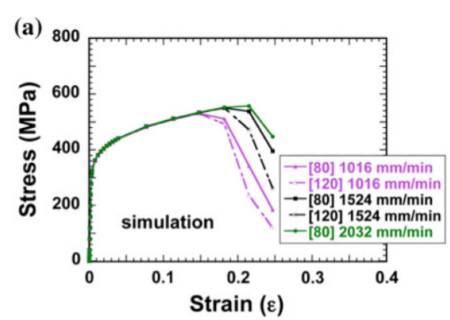

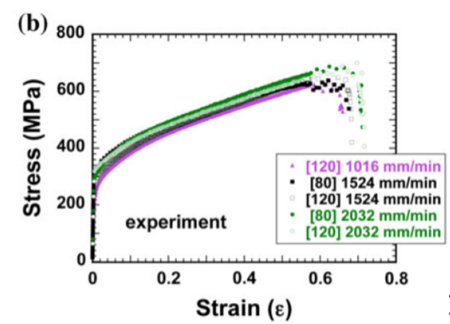

*Madison, Aagesen, Battaile, Rodelas, Payton, **MMA,** Vol. 2 (2013) pp. 359-363*

Mechanical Response II

Empirically Informed Ideal Cases

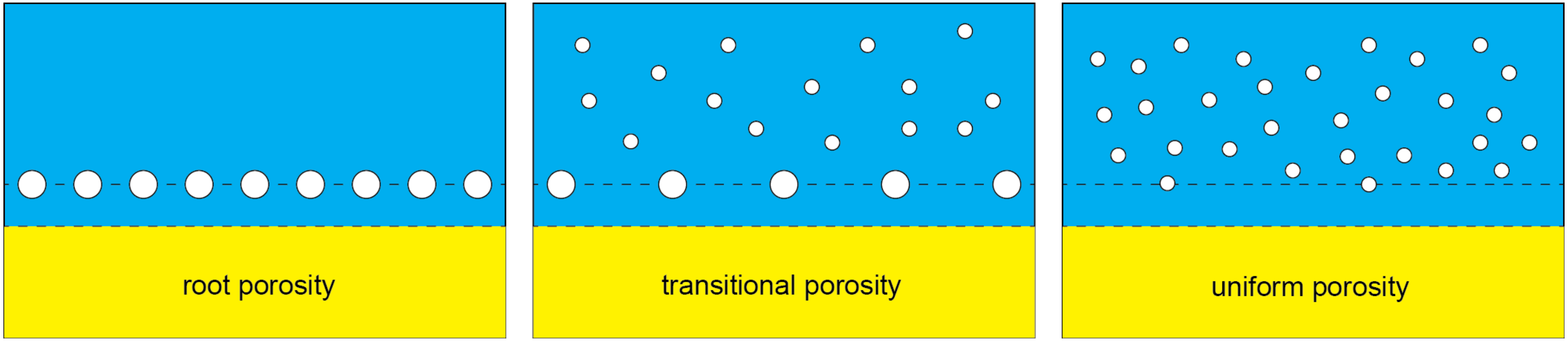

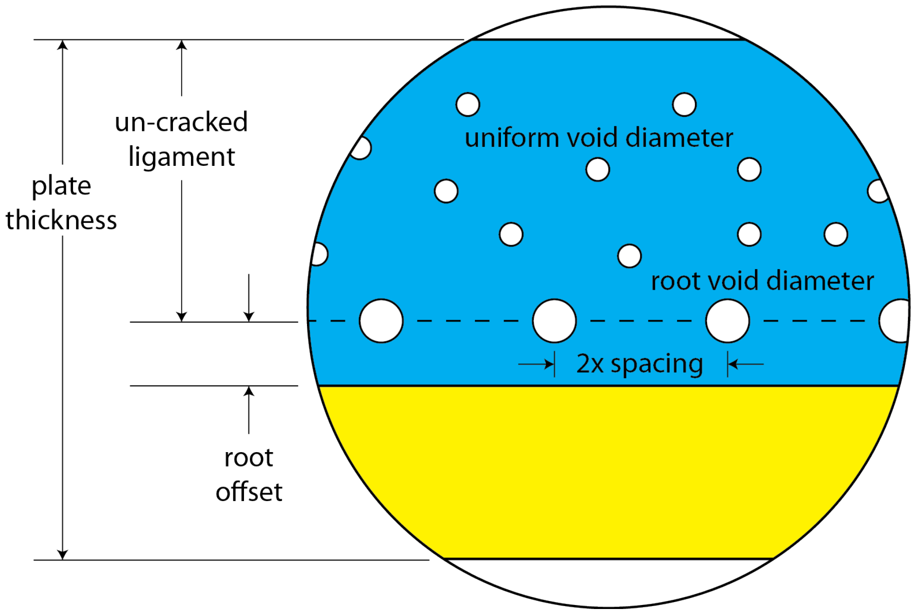

plate thickness: 0.090 in., 2.29 mm
un-cracked ligatment: 0.060 in., 1.52 mm
root offset: 280 microns
root void diameter: 191 microns
uniform void diameter: 95.2 microns
root void spacing: 1D, 191 microns
common area fraction: 0.049

Root porosity is uniformly distributed - uniform porosity is randomly distributed. ☺

Mechanical Response III

Characteristic measures

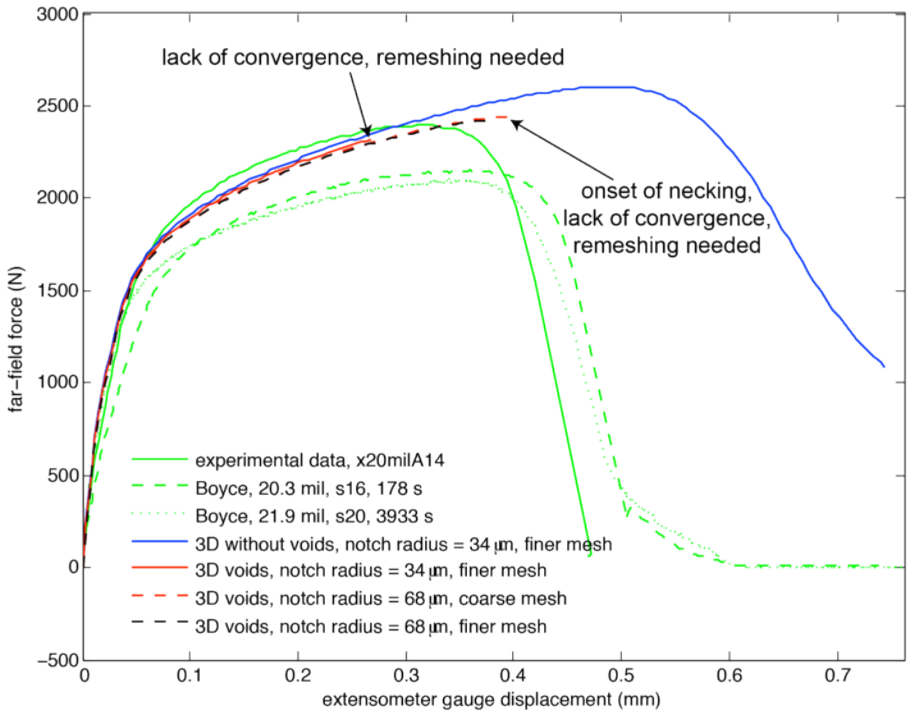

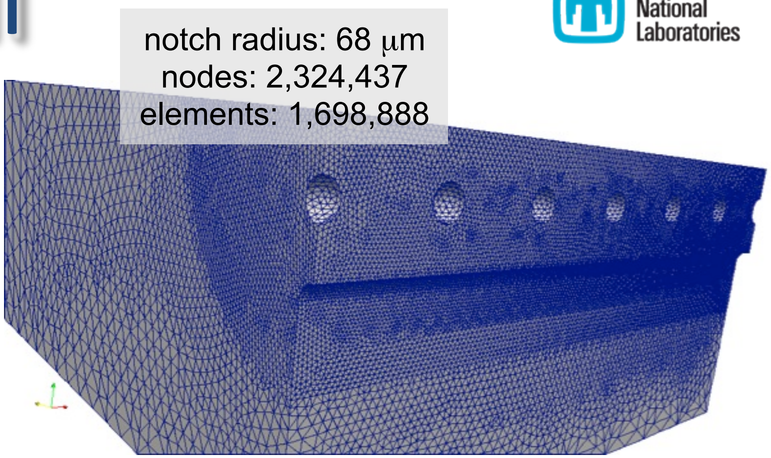

Sheet thickness: 1.6 mm
Ligament length: 508 μm
Number of voids: 6
Void diameter: 150 μm
Area fraction: 0.066 (~target)
Location: centerline of ligament
Coarse element size: 24 μm
Finer element size: 12 μm
Element type: composite-tet (10 nodes)

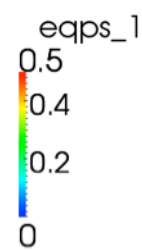

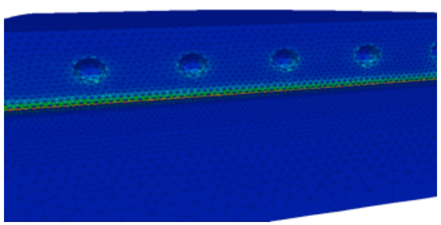

t = 0.20 s

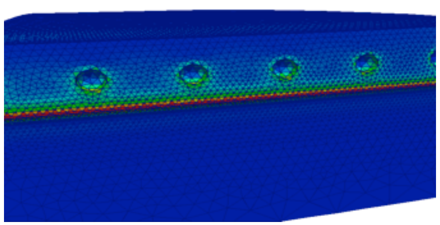

t = 0.40 s

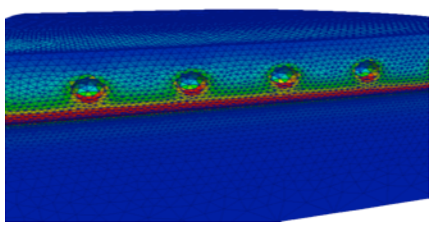

t = 0.60 s

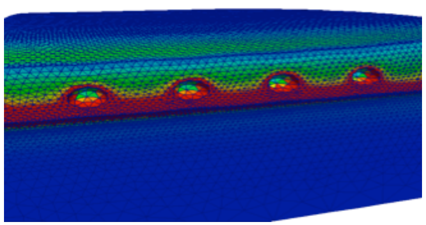

t = 0.86 s

Summary

- Average and maximum pore volume increases with decreases speed or increasing power
- Pore frequency can be reduced by increasing power beyond a speed specific threshold
- ISDs and INDs illustrate pore shape and directionality are qualitatively and quantitatively similar for a given welding speed despite power delivered
- ISDs show pore shapes are nearly spherical or ellipsoidal at low and high travel speeds and are far more irregular at moderate travel speeds.
- INDs show pore orientations become anisotropic at moderate to high travel speeds with large concentrations of pore interfacial normals pointing toward and away from the direction of laser incidence.
- Characteristic pore interspacing is nominally equivalent to characteristic pore diameter for welds with a broad range of process parameters, as reflected in the solid linear fraction (SLF) values.
- A predictive model for instantiation of pore quantity, size and their distributions has been developed based on experimentally characterized laser welds of 304L SS
- Preliminary modeling and experiments both show while smaller collections of pore volumes may significantly outnumber larger pores, smaller collections can sustain greater strains and accommodate higher stresses, even when spaced similarly as larger pore collections

Questions?

1. J. Madison, L.K. Aagesen, V.W.L. Chan, K. Thornton, *"Advancing Quantitative Description of Porosity in Autogeneous Laser-Welds of 304L Stainless Steel"* **INTEGRATING MATERIALS AND MANUFACTURING INNOVATION**, **(2014)** vol. 3, issue 11

2. J. Madison, L. K. Aagesen, C. C. Battaile, J. M. Rodelas, T. K. C. S. Payton, *"Coupling 3D Quantitative Interrogation of Weld Microstructure with 3D Models of Mechanical Response"* **METALLOGRAPHY, MICROSTRUCTURE AND ANALYSIS, (2013)** vol. 2, issue 6, pp. 359-363

3. J. Madison, L. K. Aagesen, *"Quantitative Characterization of Porosity in Laser Welds of Stainless Steel"* **SCRIPTA MATERIALIA, (2012)** vol. 67, pp. 783-786

4. J. Madison, L. K. Aagesen, Porosity in Millimeter-Scale Welds of Stainless Steel: Three-Dimensional Characterization SANDIA REPORT, **SAND2012-4474**, **(2012)** *issued by* Sandia National Laboratories, operated for the U.S. DoE by Sandia Corporation